Hindawi
Mobile Information Systems
Volume 2022, Article ID 1832836, 13 pages
https://doi.org/10.1155/2022/1832836

Research Article

Mining Engineering Image Recognition Method Based on Simulated Annealing Algorithm

Nianhua Qu, Yubiao Yan, Tong Cheng, Yajun Wang, Xin Song, and Limin Wang

School of Modern Manufacturing Engineering, School of Resources Engineering, Heilongjiang University of Technology, Jixi, China 158100

Correspondence should be addressed to Nianhua Qu; qunianhua@hljshljgyhy999.onexmail.com

Received 22 February 2022; Revised 15 March 2022; Accepted 22 March 2022; Published 11 May 2022

Academic Editor: Hye-jin Kim

Because the current methods used in mining engineering image feature recognition have some problems, such as poor classification accuracy, operation efficiency, and inability to recognize rotation features, in order to promote the development of mineral processing in China and improve resource recovery, simulated annealing algorithm is applied to the process of mining engineering image feature extraction in this paper. Based on the simulated annealing algorithm, this paper introduces the image recognition technology based on the simulated annealing algorithm and uses this image recognition technology to study the separation of ore and rock according to the differences between ore and waste rock in morphology and R, G, and B primary color components. At the same time, based on the local binary mode theory, the local variance of pixels is calculated successively to obtain the variance diagram of mining engineering image. At the same time, the simulated annealing algorithm is used to calculate the vector in each direction in the variance diagram of mining engineering image, and then, the vector is combined as the image eigenvalue. The obtained eigenvalue is combined with the binary pattern feature to realize mining recognition method and feature recognition. Finally, the experimental research shows that the algorithm proposed in this paper can quickly extract the spatial data information of mining engineering image variance and reuse the information of image local binary pattern. Compared with the traditional mining engineering image feature extraction algorithm, the recognition accuracy of this algorithm can reach 85%.

1. Introduction

There are many nonlinear recognitions in mining, various functions, and big differences. These features will be more prominent in the subsequent development. During the image recognition of mining engineering image, we have learned about China's modern mining culture [1–3]. This series of problem solving is the key to how to carry out the nonlinear identification and analysis of the mining design plan. The current nonlinear identification analysis method is dominated by expert review and qualitative nonlinear identification analysis. Delphi method and analytic hierarchy process are used to clarify the index weight method of nonlinear identification analysis, and the effect is obvious. Of course, there are shortcomings, which will lead to subjective errors in the results of nonlinear recognition analysis. This error is unavoidable and will gradually increase with the rating level. Therefore, the feasibility of using fuzzy upper-lower-level functions to identify and analyze nonlinear schemes needs further research. According to the difference of the nonlinear recognition analysis of mining design and the nonlinear relationship of the corresponding elements, the theory and method of system analysis are proposed, the comprehensive nonlinear recognition analysis model is established, and the comprehensive nonlinear recognition analysis of the mining design scheme is performed. In recent years, in the application of the situation, researchers have also proposed a nonlinear comprehensive model that quickly digests the knowledge and experience of experts [4, 5].

The rapid development of mineral resources mining and processing technology provides a strong material foundation for the construction of China's national economy, but China's mineral raw material processing technology still lags behind developed countries. The separation of ore and waste

rock after mineral mining is the first process of mineral processing, which has a profound impact on the efficiency and effect of mineral processing. Ore and waste rock preseparation plays an important role in mineral processing technology, especially in the case of China's increasingly depleted mineral resources, increasingly fierce market competition, and increasingly prominent environmental problems; how to make full use of limited resources, improve enterprise market competitiveness, and reduce the damage to the environment has become the primary consideration of mining enterprises. At present, the separation methods of ore and waste rock adopted by Chinese beneficiation enterprises mainly include heavy medium separation, dry magnetic separation, and X-ray fluorescence beneficiation. These beneficiation technologies need manual control and belong to manual detection, with poor stability, low precision, and efficiency. Therefore, it is urgent to study the ore waste rock separation technology with high degree of automation. China is rich in engineering resources. As the most important strategic resources, engineering plays an important role in economic development. In the process of engineering mining, the mixing of gangue greatly affects the use efficiency of coal. Engineering separation is an indispensable link in the process of engineering utilization. Machine vision technology has the characteristics of strong universality and easy implementation. It can realize noncontact detection and is conducive to environmental protection. It is suitable for the repetitive industrial production of engineering mining. The key of engineering recognition is how to effectively express the engineering image features. The quality of feature extraction will directly affect the results of classification and recognition. Yu Guoming and others proposed a method of coal and gangue image recognition using gray value, but it needs certain auxiliary conditions, and the process is complex [6, 7]. The engineering image feature extraction method proposed by Wang Xiangrui is relatively simple, but the feature extraction method based on gray value is single, which affects the recognition accuracy in the specific environment of coal mine and cannot meet the actual needs. He Min et al. used the feature extraction method of gray level co-occurrence matrix. Because the extracted feature parameters are relatively few, it is easy to affect the recognition results. Liao Yangyang and others used BP network recognition method. Due to the influence of experimental sample differences, its recognition accuracy is not high. Moreover, the above feature extraction methods are difficult to adapt to the classification and recognition in the actual environment, and the accuracy needs to be improved. Therefore, it is necessary to study the feature extraction methods that can accurately describe the engineering image. In recent years, simulated annealing algorithm has been widely used in image denoising, face recognition, image restoration, image super resolution, and image classification. Because of its sparse representation, simulated annealing algorithm increases the number of simulated annealing atoms and enriches their morphology, which can better match the structure of signal or image itself. The simulated annealing algorithm is used to extract the image features of the project. After randomly selecting the sample image of the project as the simulated annealing atom, the learning simulated annealing is updated randomly in the order of columns, so as to effectively express the image features of the project to the greatest extent and improve the efficiency of recognition [8].

In this paper, the simulated annealing algorithm is applied to the image recognition process of mining engineering. The difference from the classic algorithm is that a random method is selected in the process of simulating and initializing the image features of mining engineering and collecting data. Mainly by taking the mining engineering image feature extraction as the simulation initial quantity in the initialization process, the features of the mining sample image can be effectively extracted in the process of image recognition according to a certain sequence [9, 10].

2. Basic Technology and Related Algorithm

With the widespread use of simulated annealing algorithms in different industries, image features can be expressed as a linear combination of original features. The simulated annealing algorithm method can complete the extraction and recognition of mining engineering image features by optimizing the corresponding cost function. The analog quantity $D = [d_1, d_2, \cdots, d_q] \in R^{p \times q}$ is given to the process of extraction and recognition, each column $d_k \in R^p$ in the analog quantity D is called a feature quantity, and the image feature can be expressed as the linear combination of several feature quantities in analog quantity D. $Y = [y_1, y_2, \cdots, y_s] \in R^{p \times s} Y \approx DXX = [x_1, x_2, \cdots, x_s] \in R^{q \times s}$ It is the corresponding coefficient of variable Y under analog quantity D. X vectors all have characteristics, and the relevant elements contained in the vectors can be obtained, so X is called a variable matrix [11].

In the mining image recognition of the simulated annealing algorithm, the variable Y can be regarded as the image feature of the mining engineering image, D is the simulation learned from the mining sample image, and X is the representation coefficient of the mining engineering image variable Y under the simulated quantity D. The simulated annealing algorithm is the process of solving D and X. The simulated annealing algorithm problem corresponding to this process can be described as

$$\min_{D,X} \left\{ \| Y - DX \|_F^2 \right\} \quad s.t. \quad \forall i, \|x_i\|_0 \le T_0, \tag{1}$$

where Y represents the image feature matrix of mining engineering images; $x_i\}$ represents any vector in the variable matrix X; $\|\cdot\|_F$ represents the F norm; $\|\cdot\|_0$ represents the norm corresponding to L_0; and T_0 represents the initial value set, which is affected by the feature similarity.

In order to solve the above problems, this paper uses the simulated annealing algorithm to calculate in two steps, setting the analog quantity D and the variable matrix X, respectively, and using the loop operation to solve the other variable, it runs until the convergence value of the algorithm or the set frequency of operations. Therefore, the calculation process is mainly divided into two stages: the first stage is the

Input:Sample matrix $Y = [y1, y2, y3] \in RP * s$
Dictionary $D = [d1, d2, \cdots., dq] \in Rxq$
Output:Sparse matrix $X = [x1, x2, \cdots .x,] \in Rq * s$
(1)$i = 1$.
(2)$r^0 = y^i$, $\Omega = \bigcirc$, $k = 1$
(3)$jk = \text{argmax}|\langle rk - 1\rangle|$, $j = 1, 2, 3, \cdots, q$
$\Omega^{\text{k}} = \Omega^{\text{k}-1}$, $U\{jk\}$
(4)$x^k = \text{argmax}|yi - D_\Omega ix|2$,
$D = [dw1, dw2, \cdots .dwk], w1, w2, \cdots, wk \in \Omega k$
(5)$rk = yi - D_\Omega r\, xk$
(6)If $I|r|2<\&2pork>aq$, go to step(7)
Otherwise $k - k + 1$,repeat step(3)–step(5)
(7)The t-th element in the vector $x\, i(t) = x * (t), t \in S2r$
(8)If $i < s$,then $i = i + 1$, repeat steps (2)–(7)
Otherwise, output $X = [X1, X2, \cdots X3]$

Algorithm 1: Feature extraction algorithm flow.

extraction of numerical features; that is, the analog quantity D is set, and the value of the variable matrix X is calculated using the OMP algorithm. The detailed calculation steps are shown in step (3) in Algorithm 1. In order to solve the relevant column number of the residual r, step (4) is to use the least square method to calculate the data sample image; step (5) is the algorithm to identify the residual r of the image feature; and step (6) is the constraint condition for the end of the algorithm execution. The second stage is the recognition of image features; that is, the variable matrix X is used to sequentially recognize the analog quantity D. Suppose the kth column d_k corresponding to the image analog quantity D to be recognized, and the kth row of the product of the variable matrix X and d_k is x_T^k, then the objective function of the mining engineering image can be expressed as

$$\begin{aligned} \|Y - DX\|_F^2 &= \left\| Y - \sum_{j=1}^{q} d_j x_T^j \right\|_F^2 = \left\| \left(Y - \sum_{j \neq k} d_j x_T^j \right) - d_k x_T^k \right\|_F^2 \\ &= \left\| E_k - d_k x_T^k \right\|_F^2, \end{aligned} \tag{2}$$

where $E_k = Y - \sum_{j \neq k} d_j x_T^j$ represents the error value caused by removing the corresponding part of the feature quantity d_k in all samples.

In order to ensure the feature vector of the image, it is not necessary to calculate and solve the SVD for E_k, and it can be converted by E_k and x_T^k. $E_k \longrightarrow E_k^R$, $x_T^k \longrightarrow x_R^k$, x_R^k are made to represent the elimination of 0 elements in x_T^k, and only save nonzero elements; E_k^R means that only the corresponding d_k in E_k and the nonzero elements in x_T^k are saved for the product item. The initialization function can be transformed into $\|E_k^R - d_k x_R^k\|_2^2$, where the F norm in the function can be represented by L_2 norm. It is necessary to perform SVD solving operation on E_k^R, get $E_k^R = U\Delta V^T$, and identify the kth column of the simulation process. d_k denotes the first column of U element; identification x_R^k represents the corresponding product of the first column element of V and Δ (1,1). That is, the recognition of the feature quantity of the analog quantity D can be realized [12]. The simulated annealing algorithm realizes the initialization of the analog quantity D in the process of extracting image features. It adopts a random selection of different samples for conversion, and the process of identifying image features is completed in a sequence of columns. However, the results obtained by the initialization and identification of different analogs are quite different. In the initialization process of image feature vector simulation, this paper randomly selects different samples as the feature values of the simulation variables according to the training samples and obtains the recognition rate of mining image features through multiple operations.

2.1. Fundamentals of Image Feature Recognition in Mining Engineering. The image recognition system of mining engineering mainly distinguishes the mining industry based on the characteristics of the mining image. These differences vary according to the physical properties of coal and rock, such as color, gloss, port, and section characteristics. Among them, the image features of coal and floor slate are very different, which is the best attribute for image classification of coal and rock [13].

The current mining mainly consists of bituminous coal and anthracite. Floor slates are mainly sandstone and mudstone (Figure 1).

As one of the natural features, the mine features show irregularities, strong randomness, moderate extraction of target feature dimensions, strong discrimination ability, good robustness, and small calculation requirements. Considering these factors comprehensively, the concept of simulated annealing based on statistical methods is proposed, and a mining engineering image feature extraction algorithm based on simulated annealing algorithm is proposed.

2.2. Image Feature Extraction Algorithm. First, calculate the local dispersion of each pixel within the framework of the local binary pattern theory, and then, use the simulated annealing algorithm to extract image features from the local dispersion diagram, and merge and classify the final extracted features with the simulated annealing features to realize the recognition of for image features in the mining process.

During the calculation of simulated annealing, the simulated annealing value of the pixel is calculated by comparing the relative size of the gray value of the adjacent point and the center pixel; although it can be realized, this process makes the simulated annealing operator lose the ability to describe the relative size of the value gray value of the center pixel. The local variance is an effective parameter to describe numerical information. The local variance of a pixel is defined as the variance of the gray difference between multiple adjacent points and the central pixel in the simulated annealing calculation and is the variance of the local binary mode. The local binary patterns variance (LEPV) algorithm uses local variance. However, there are many shortcomings in simulated annealing V, and the spatial distribution

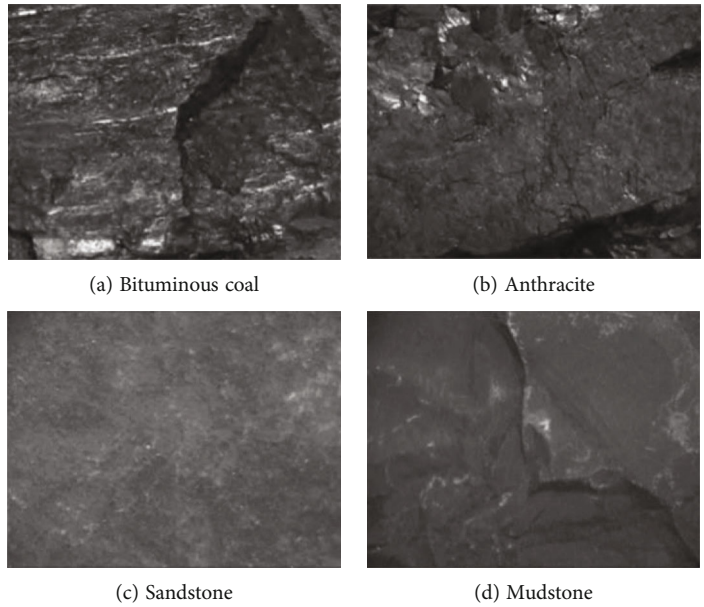

(a) Bituminous coal (b) Anthracite

(c) Sandstone (d) Mudstone

Figure 1: Feature images of some mining samples.

relationship of local dispersion is not specifically considered. Experiments show that different types of features have different spatial distributions of local dispersion, and the features extracted from the spatial distribution relationship of local dispersions can be used for feature recognition [14, 15].

In view of the circular area with the pixel of any mining engineering image as the center, assuming that the radius of image recognition is R, the gray value corresponding to the center pixel is expressed as g_c, which can be evenly distributed on the circumference. The gray values corresponding to the n neighboring points are expressed in turn as $g_0, g_1, \cdots, g_{n-1}$, and then, the regional feature T can be expressed as:

$$T = t(g_0 - g_c, g_1 - g_c, \cdots, g_{n-1} - g_c). \tag{3}$$

If the simulated annealing operator is used to describe T, a symbolic function can be used to express it. The expression is shown in Equation (4), where $s(x)$ represents a symbolic function.

$$T = t(s(g_0 - g_c), s(g_1 - g_c), \cdots, s(g_{n-1} - g_c)), \tag{4}$$

$$s(x) = \begin{cases} 0, & x < 0 \\ 1, & x \geq 0 \end{cases}. \tag{5}$$

Use variance to express the local features of the image using T as:

$$T = V(K) = V(g_0 - g_c, g_1 - g_c, \cdots, g_{n-1} - g_c), \tag{6}$$

where $V(K)$ represents the variance of the elements in the operation set K.

When assigning a value to the central pixel of the image, the central pixel value of the corresponding image becomes the local dispersion value $V(g_0 - g_c, g_1 - g_c, \cdots, g_{n-1} - g_c)$. The local variance at pixel k is represented by var (k).

When calculating the local variance of the pixels of all images, a local variogram is obtained and calculated in the theoretical framework of simulated annealing, so it is also called a simulated annealing variogram. Figure 2 shows the local distribution map of different types of coal and rock feature images.

In the local dispersion diagram, the variance larger the pixel value, the more conspicuous the contrast of the gradation values between the pixels in the local area centered on the pixel. Generally, the greater the local dispersion of the boundary, the smaller the local dispersion in the region where the gray level changes slowly. The spatial distribution of the local dispersion reflects the spatial distribution of the features. This is also the theoretical basis for the simulated annealing algorithm to extract image characteristics. It can be seen from Figure 2 that the characteristic structures of the local dispersion maps of coal and rock are quite different.

The local variogram includes some feature information, and the simulated annealing algorithm is used to extract this feature information and process them.

The simulated annealing algorithm is also called half-side difference graph. The simulated annealing algorithm is to set the step size as a parameter function and form a set of pixel gray difference in a certain step in a certain direction of the gray image. Half of the dispersion of the element value of this group is the simulated annealing algorithm value in this step. By modifying the steps, multiple function values corresponding to the step length can be obtained. Through the approximate calculation of successive steps, the simulated annealing algorithm curve is obtained. The calculation of the simulated annealing algorithm, as shown in Figure 3, is the combination of the pixel pairs when the steps h of the solid line and the dashed line are 1 and 2.

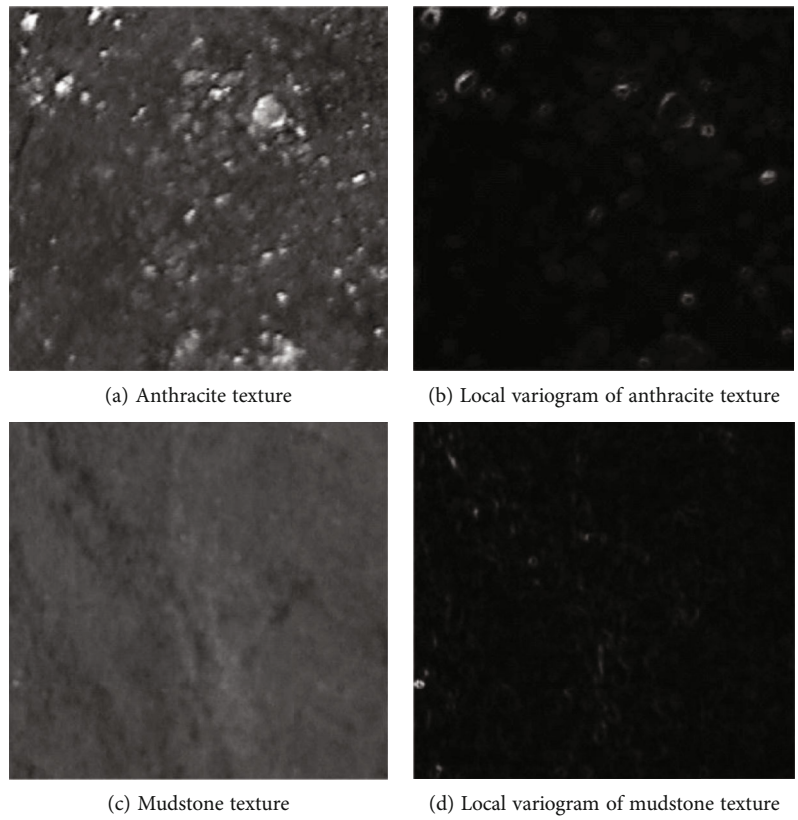

(a) Anthracite texture (b) Local variogram of anthracite texture

(c) Mudstone texture (d) Local variogram of mudstone texture

Figure 2: Different mining feature images and their local variogram.

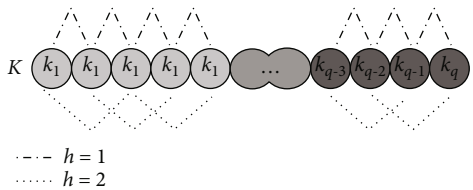

Figure 3: Calculation of simulated annealing algorithm.

K is used to this feature information represent a collection of pixels distributed in a certain direction in the mining engineering image, and then, the number of pixels in the this feature information set K of pixels can be represented by q, and then, the pixel k_i corresponds to the i-th pixel in the set K. The corresponding image gray value is represented by {O3jc}{S3g}{S3h}, the step size is set to h, and the expression for calculating $r(h)$ is

$$r(h) = \frac{1}{2N(h)} \sum_{i=1}^{N(h)} [g(k_i) - g(k_i + h)]^2, \tag{7}$$

where $N(h)$ indicates that the pitch step h pixels in the set K are expressed by $N(h) = q - h$.

According to expression (7), it can be seen that the variance after using the simulated annealing algorithm is reduced to half of the original.

Convert the image gray value $g(k_i)$ in expression (7) into the local variance of the image var (k_i), and then, the operation expression in the local variogram can be obtained as

$$r(h) = \frac{1}{2N(h)} \sum_{i=1}^{N(h)} [\text{var}\ (k_i) - \text{var}\ (k_i + h)]^2. \tag{8}$$

Under the simulated annealing algorithm, the feature complexity of mining images in different regions is dynamically adjusted to appropriate parameter values. The simulated annealing algorithm strengthens the nonlinear recognition analysis of small targets, referring to the feature pyramid network (FPN) [16, 17]. Combining the front-end features and the shallow feature information, a multiscale fusion method is adopted, and the location and class predictions are made with feature maps of multiple scales. The nonlinear identification and analysis of the industrial and mining joint mining design scheme are deeply studied. In the design of the comprehensive nonlinear identification and analysis mathematical model, based on the principles of mining technology and economics and the theoretical methods of system analysis, the nonlinear relationship between nonlinear identification and analysis of the elements is considered, to establish the multifunctional comprehensive profit evaluation model for the mining joint mining design scheme.

In the case that the selected direction is not the axial direction, firstly, refer to the center pixel of the subimage

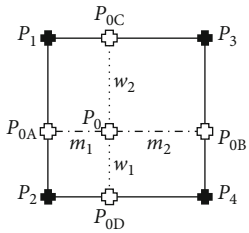

Figure 4: Bilinear interpolation.

to determine the position of the direction corresponding to the subpixel and its nearby points, and then, calculate the gray value of adjacent points through bilinear interpolation. Furthermore, the local dispersion corresponding to the subpixels is obtained. Finally, the simulated annealing algorithm is calculated in the local dispersion group of subpixels in this direction. $P1$, $P2$, $P3$, and $P4$ are set as four adjacent pixels $P0$ distributed in a square corner relationship in space, which are any subpixels in the square area or on the boundary. The distance between P0 and the square boundary is $m_1 m_2 w_1$, w_2, and the corresponding points on the boundary are shown below. $P_{0A}P_{0B}$, P_{0C}, and P_{0D} are shown in Figure 4.

Knowing the local variance of $P1$, $P2$, $P3$, and $P4$, then, the local variance of the subpixel P0 can be calculated as

$$P_0 = \frac{m_2 w_1}{(m_1 + m_2)(w_1 + w_2)} P_1 + \frac{m_2 w_2}{(m_1 + m_2)(w_1 + w_2)} P_2 + \frac{m_1 w_1}{(m_1 + m_2)(w_1 + w_2)} P_3 + \frac{m_1 w_2}{(m_1 + m_2)(w_1 + w_2)} P_4. \tag{9}$$

When the simulated annealing algorithm values in the corresponding directions of the multiple subimages are averaged, the target feature vector and the vectors in the multiple directions are obtained to form a matrix of simulated annealing algorithm. There are two methods for calculating target image features through simulated annealing algorithm matrix. One is to calculate the simulated annealing algorithm parameters in different directions through matrix fitting of the simulated annealing algorithm. As an image feature, the analytical effect of this method is limited, with large calculated amount. Another method is to sequentially connect each direction vector in the simulated annealing algorithm matrix to obtain the final image feature, and compared with the first method, this method is simpler and more effective, so this method is adopted in this paper. As shown in Figure 5, the process of extracting image features from the local dispersion map through the simulated annealing algorithm selects four directions of 0.45, 90, and 135° to calculate the simulated annealing algorithm, where the angle refers to the angle between the corresponding direction and the positive direction of the axis.

The image features of mining engineering obtained by using the simulated annealing algorithm are mainly to reuse the lost information data of the simulated annealing algorithm. In order to ensure better results in the mining feature

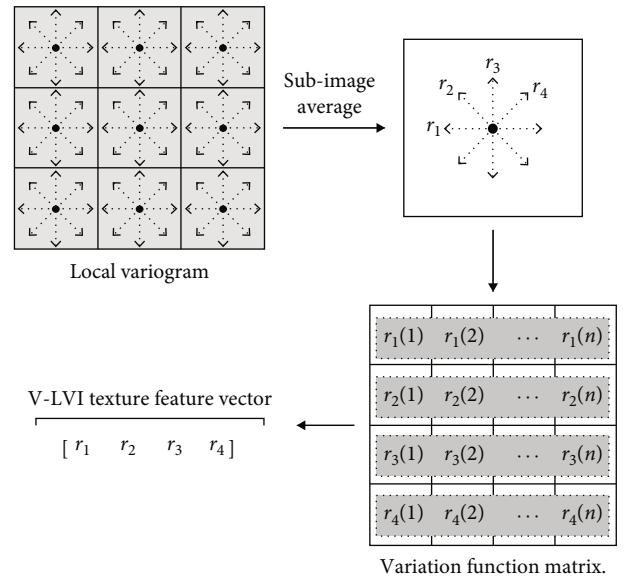

Figure 5: Image feature extraction process based on simulated annealing algorithm.

image classification process, it is necessary to use this algorithm to extract image features and simulated annealing algorithm feature for fusion.

Feature fusion is in the process of calculating the feature similarity of the mining image. First, this algorithm is used to extract the feature similarity of the image in turn, and the fusion coefficient is used to determine the image similarity. The features obtained by the simulated annealing algorithm can be represented by histogram features, then the image similarity can be represented by the histogram distance, and then the operation expression is

$$D_C(X, Y) = \sum_{i=1}^{n} \frac{(X(i) - Y(i))^2}{X(i) + Y(i)}. \tag{10}$$

The feature obtained by the simulated annealing algorithm is that the function value corresponding to the step size can basically reflect the feature information of the mining image, and in this paper, the austenite distance is used to express the similarity of the image. The training sample and the test sample are represented by X and Y, respectively. X_1 and Y_1 can represent the feature vector obtained by using the simulated annealing algorithm, that is, the feature similarity of the mining image.

$$D = \alpha D_1(X_1, Y_1) + (1 - \alpha) D_2(X_2, Y_2), \tag{11}$$

where, in the expression, D reflects the different similarities of the two samples of X and Y. If D is larger, the similarity of the image will be smaller; $D_1(x, y)$ and $D_2(x, y)$ indicate the Chi-square distance and the Euclidean distance in turn; α indicates the fusion coefficient. If $0 < \alpha < 1$, then the recognition can be improved by changing the value of α effect.

In this paper, the vector sequence of the matrix under the simulated annealing algorithm is connected to obtain

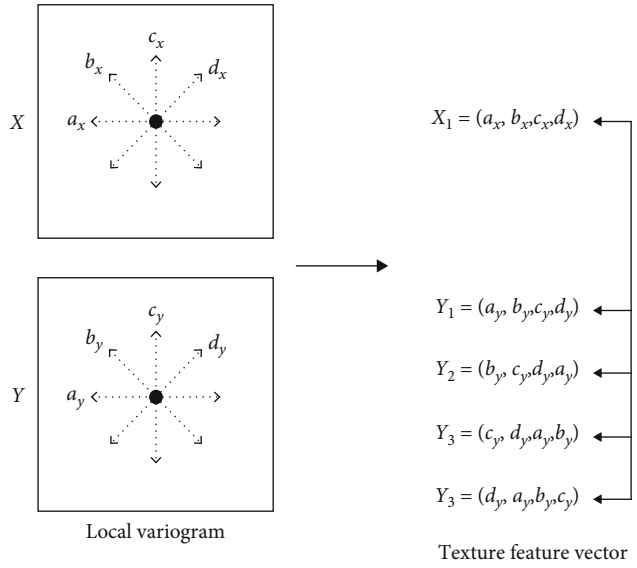

Figure 6: Directional relationship of vectors a.

the feature vector of the image, but the image feature obtained is very poor in rotation, especially the feature under different direction changes. The vectors can be connected in a certain order, and the similarity of the images can be calculated, in order to describe in detail, as shown in Figure 5. For the training sample$X$and the test sample Y, sequentially calculate their corresponding four direction vector values a_X, b_X, c_X, and d_X, and a_Y, b_Y, c_Y, and d_Y are shown in Figure 6; the corresponding relationship of each vector direction is connected to each vector in turn from the beginning of the training sample X to obtain the feature vector X_1, and for the test sample Y, $a_X a_Y b_Y$, c_Y, and d_Y are connected, respectively, to obtain different feature vectors Y_1, Y_2, Y_3, and Y_4 in a certain order, and these four feature vectors form a rotating feature vector group. Calculate the similarity between each vector in the rotation feature vector group and Xi, respectively, and the minimum value is the similarity between sample Y and X, namely

$$D(X, Y) = \min\left[(X_1, Y_1), (X_1, Y_2), (X_1, Y_3), (X_1, Y_4)\right]. \tag{12}$$

The more calculation directions of the simulated annealing algorithm, the stronger the descriptive ability of the rotation characteristics of the simulated annealing algorithm, which increases the calculated amount accordingly.

The features extracted by the simulated annealing algorithm are classified as simulated annealing features. The flow of the simulated annealing algorithm is shown in Figure 7. The classification process realizes feature fusion, and the image characteristics are rotation invariant.

3. Analysis of Experiment and Results

In order to verify the effectiveness of the simulated annealing algorithm applied to the feature recognition of mineral deposits, typically, sandstone and mudstone of coal samples

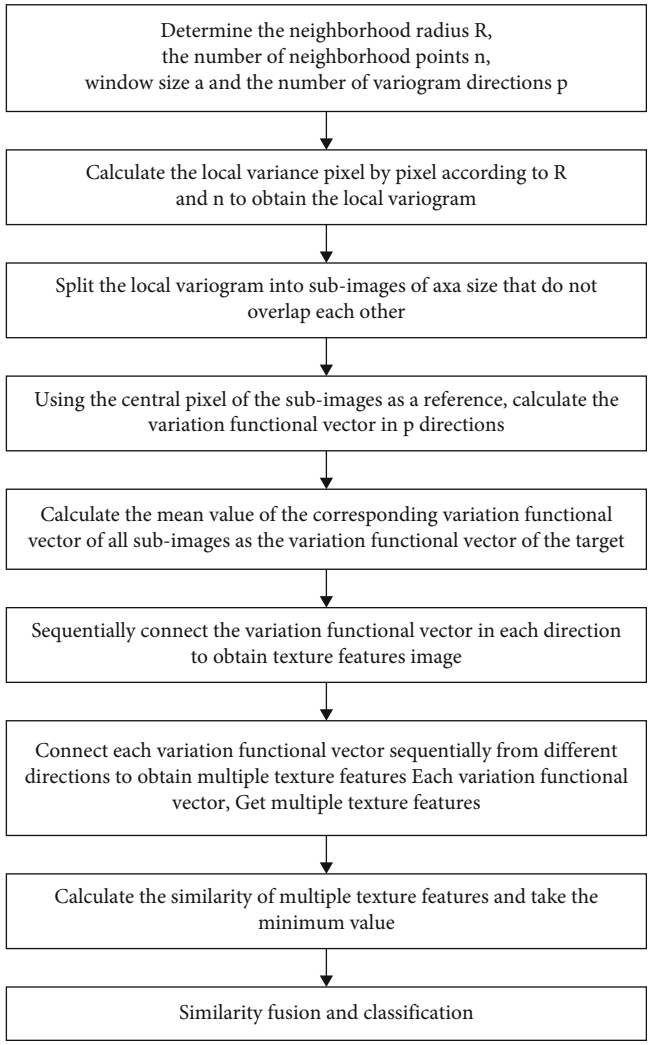

Figure 7: The flow of simulated annealing algorithm.

are selected as rock samples to form a feature image sample database of the mining industry for feature extraction and identification testing in this paper.

Select 208 samples, and randomly select 39 images from each level of 52 images of coal, anthracite, shale, and sandstone into the training group. The remaining 13 images are used for testing. Here, coal and anthracite are one kind, representing coal. Another kind is sandstone and shale, which are used as representative rocks. Meanwhile, only one-half of mining is done. The total image size of each mining sample is 48×48, the format is png, and the gray level is 256.

The images of mining engineering collected in mines are affected by the environment, and the image quality of mining projects is mainly affected by factors such as light intensity, mine dust interference, and mechanical vibration. In this paper, the specific effects of these factors are not researched, but images of mining industry samples are collected, and experiments with different light intensities are conducted. As shown in Figure 8, each of the 4 images of sandstone, anthracite, soot, and shale are collected with different light intensity, and the range of light intensity was not large.

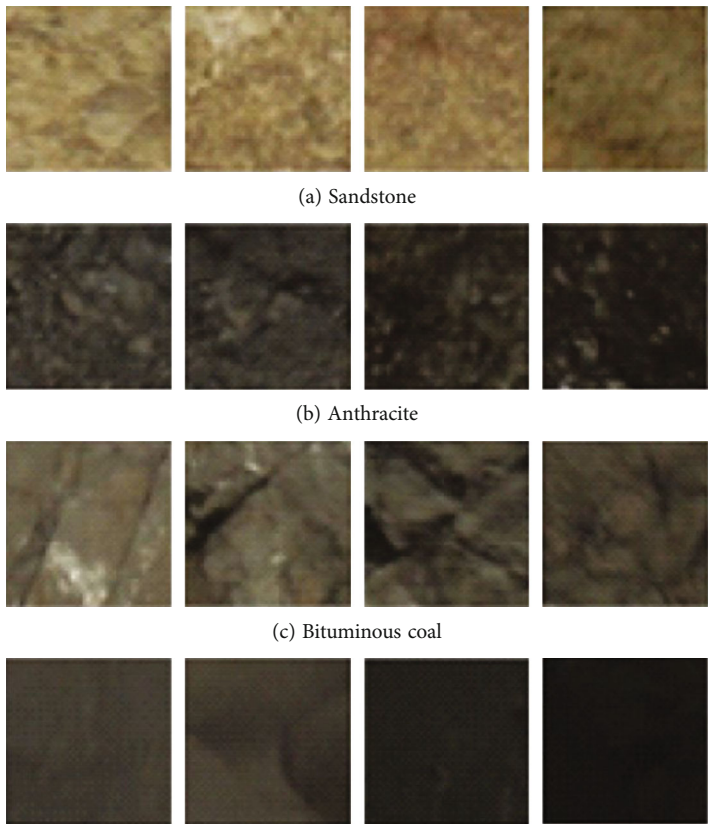

(a) Sandstone

(b) Anthracite

(c) Bituminous coal

(d) Shale

Figure 8: Mining sample images under different lighting.

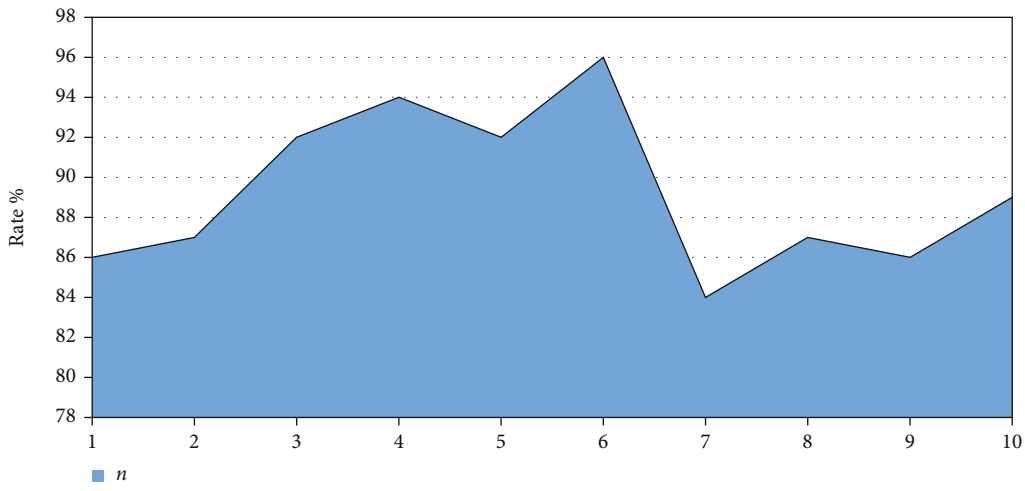

Figure 9: Recognition rate under different simulation initialization and recognition.

All experimental data in this article are obtained by Matlab 7.10.0. (R10a) test.

Each sample image of the training group is connected to a column to form a training sample matrix, and each column of the training sample matrix represents a sample image. The training sample matrix performs dimensionality reduction through the PCA algorithm to obtain the feature space matrix E, the sample image average vector m, and the training sample matrix after the dimensionality reduction. The result of the test is that when the dimensionality decreases, by keeping the feature vectors corresponding to all nonzero singular values, a better classification effect can be obtained. The training sample matrix after the elevation dimension is normalized, and even if the matrix Y is obtained, the pattern of each normalized vector is 1. Similarly, pull all test images into one column to form test sample matrix A, and project A

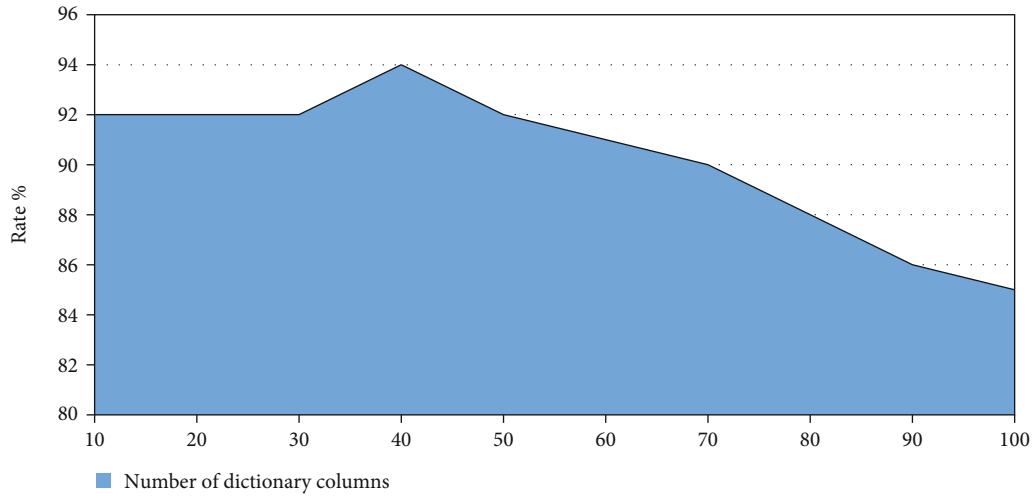

Figure 10: The relationship between the number of simulated columns and the recognition rate.

Table 1: Recognition rate under different parameter selection.

Number of simulated columns	Characteristic error (g)	Feature similarity (a)	K	Recognition rate of test sample	Number of wrong samples	Recognition time/s
42	0.038	0.3	9	0.96154	2	2.909132
40	0.038	0.3	9	0.94231	3	2.796078
60	0.027	0.19	11	0.86538	7	3.854129
80	0.042	0.41	7	0.76923	12	5.741191

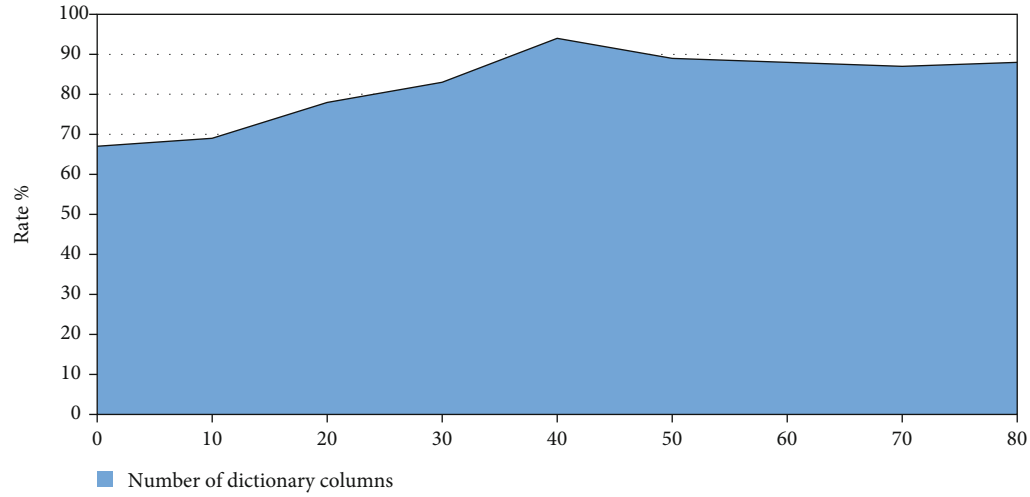

Figure 11: The relationship between feature error and recognition rate.

into feature space E to obtain matrix B. The projection formula is as follows:

$$B = E^T(A - M), M = [m, m, \cdots, m]. \quad (13)$$

Finally, the matrix B can be normalized.

In order to reduce the dimensionality of the sample image on the PCA, this step is not only needed, but also the redundant data information in the sample image is greatly removed, to reduce the time and space cost, improve the operating efficiency of the entire algorithm, and establish the foundation for subsequent simulated annealing algorithm. Otherwise, the analog quantity D contains a lot of redundant information, and the simulated annealing algorithm is invalid.

First, as shown in Figure 9, the impact of different simulation initialization and recognition methods on the recognition rate will be described. Figure 9 shows the recognition rate of test samples measured 10 times continuously under the same parameter conditions through different simulation initialization and recognition methods. The same parameter

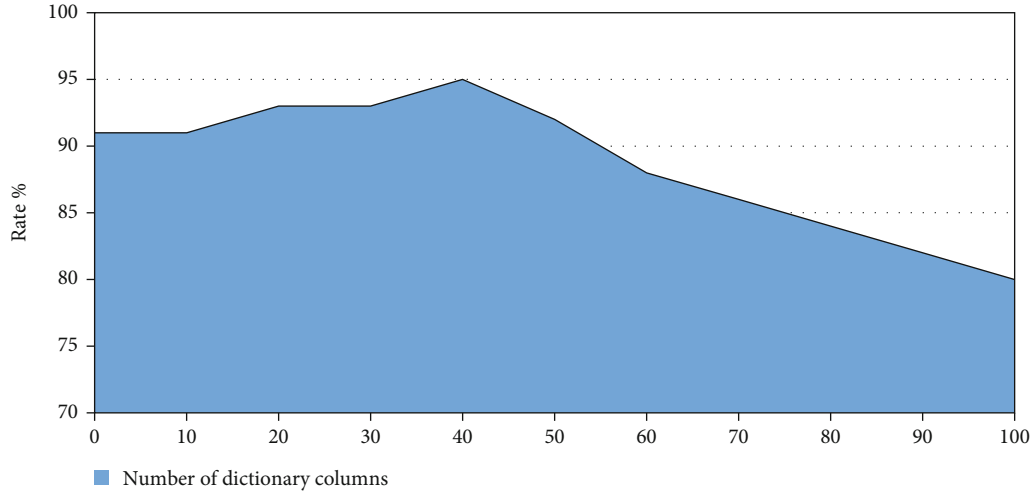

Figure 12: The relationship between feature similarity and recognition rate.

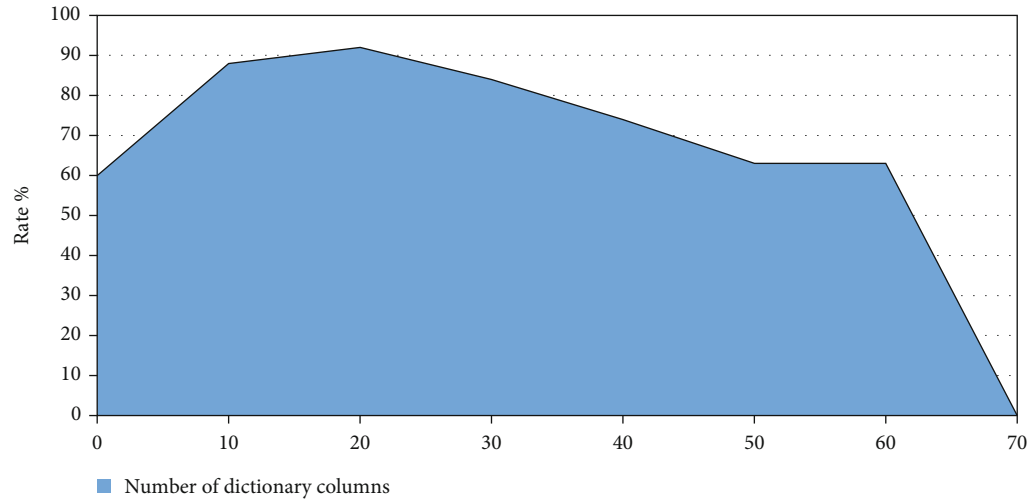

Figure 13: The relationship between K value and recognition rate.

condition here is that the number of simulated columns, feature error, and feature similarity are the same as K. As shown in the figure, different simulation initialization and recognition methods have a great impact on the recognition rate, and the fluctuation of the recognition rate reaches 10%. Under this parameter condition, the highest recognition rate among the 10 recognition rates is selected as the recognition rate. As shown in the figure, when the recognition rate is the highest for the sixth time, as the recognition rate under this parameter, the recognition rate of all the following test samples is measured.

Figure 10 is a graph showing the change curve of the mining recognition rate of different simulated column numbers under the same test condition. Here, parameter characteristic error =0.035, feature similarity =0.28, and $K = 9$. It can be seen from Figure 10 that with the gradual increase in the number of simulated columns, the recognition rate of the mining industry tends to decrease. The number of simulated columns is 70 as the branch point, and the recognition rate before 70 is relatively stable. The recognition rate of those after 70 dropped sharply. The number of simulated columns determines the dimension of the image feature vector of the mining process. The larger the number of simulated columns, the greater the time and space price for algorithm execution, which can be learned from the data in the last column of Table 1. As the number of simulation columns increases, mining identification time also increases. If the number of simulated columns is too small, the dimension of the feature vector is too small, and it is easy to be buried by image noise.

Table 2: The influence of simulated annealing algorithm on recognition rate.

Simulated usage	Recognition rate of test sample/%	Number of wrong samples
Nonuse	61.538	20
Use	96.153	2

Table 3: Mining engineering image recognition accuracy of different algorithms.

(R,n)	RI simulated annealing	U simulated annealing	Simulated annealing V	Dis simulated annealing	MS-LPCM	Simulated annealing algorithm
(3,8)	76.71	65.55	76.43	75.39	81.80	83.36
(4,8)	82.81	75.62	83.62	83.07	85.30	86.02

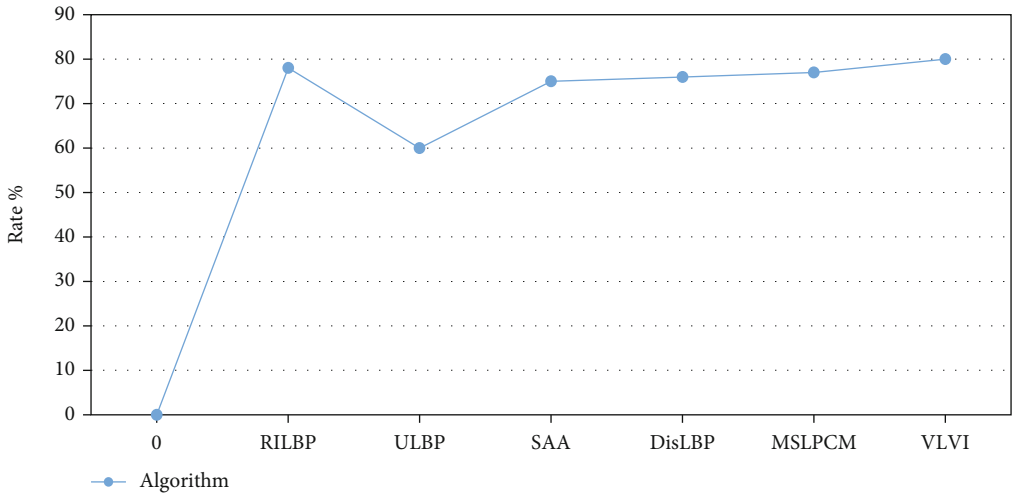

Figure 14: Histogram of mining engineering image recognition accuracy under different algorithms when $R = 3$ and $n = 8$.

The feature error is an important indicator of the feature extraction cycle of the simulated annealing algorithm. The smaller the value, the closer the sample image vector before and after feature extraction is to the austenite distance. Figure 4 is a graph showing the change curve of the recognition rate of industrial parks with different characteristic errors under the same test conditions. At this time, the number of simulated columns =40, feature similarity =0.26, and $K = 9$. In Figure 11, as the feature error increases, the training sample recognition rate tends to decrease, and the test sample recognition rate decreases after rising, and the feature error reaches a peak around 0.035.

Extracting the features of mining sample images through simulated annealing algorithm, the obtained feature vectors are not only low in dimension, but also very characteristic. Feature similarity is an important index to measure its characteristics. Figure 12 shows the relationship between feature similarity and recognition rate. The number of simulated columns =38, feature error =0.038, and $K = 9$ can be seen in Figure 12, where the recognition rate of the test sample is in the interval of feature similarity (0.1, 0.5). The above is relatively gentle, reaching a peak around 0.35, and then slowly decreasing after 0.5.

The K value is an index parameter of the classifier, and its size directly affects the classification recognition rate. Choosing an appropriate K value is the most important work of the KNN algorithm. Figure 13 is a graph showing the influence of the K value on the recognition rate. The number of simulated columns =40, characteristic error = 0.039, and characteristic similarity = 0.36, and then confirm the sample, and then, it will fall down after it is automatically raised and lowered. The interval (7, 29) is stable, but drops sharply after 30. As shown in the figure, the fluctuation of the K value has a great influence on the recognition rate of the test sample. In order to meet the requirement of the recognition rate, the K value should be used as small as possible to reduce the operation time of the algorithm and improve the operation of the program.

It is found that the pros and cons of the simulation have a great impact on the mining recognition rate. Among them, the most influential simulation parameters are simulation initialization and recognition, feature error, and feature similarity. It can be seen from Figure 13 that since the K value has a great influence on the recognition rate, the classifier also has a great influence on the mining recognition rate.

The process of simulated annealing algorithm is the process of extracting the image features of the mining process. Reviewing the entire mining recognition process, first preprocess the image of the mining process, mainly to reduce PCA. Then, the simulated annealing algorithm is used to extract the image features of the mining process. Finally, the KNN classifier is used to classify and recognize the feature vectors of mining engineering images. Table 2 shows the case of using the mining recognition rate of feature extraction without using the simulated annealing algorithm. The recognition rate of the second row of data in the table is measured by the feature extraction of the simulated annealing algorithm (that is, the process of the simulated annealing algorithm with one more than the first case). It can be seen from Table 2 that the simulated annealing algorithm is used to feature extraction of mining engineering images. Therefore, the feature extraction method based on simulated annealing algorithm adopted in this paper greatly enhances the recognition possibilities of mining engineering images,

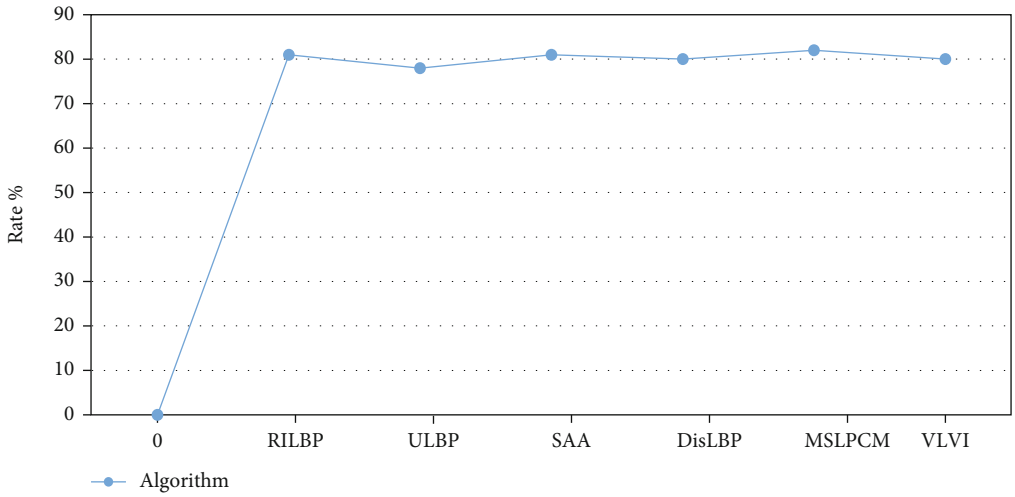

Figure 15: Histogram of mining engineering image recognition accuracy under different algorithms when $R = 4$ and $n = 8$.

can effectively express the image features of mining engineering images, and can achieve satisfactory classification and recognition results. Therefore, the method for extracting image features of mining engineering described herein can be implemented.

The original samples collected in the experiment include 112 feature images, among which the sample features are anthracite, long flame char, sandstone, and mudstone. 60 images are randomly selected from the sample data set, to perform 5 rotations of each image at random angles, and obtain 4 rotated images with a size of 180×180. It is ensured that the subimages are cut from the original image and the rotated image, and are from the same image, and any two secondary images from the same image do not overlap each other.

The combination of the simulated annealing radius and the number of adjacent points is calculated, and the experiment is repeated ten times. The average of the classification accuracy of 10 times is regarded as the final classification accuracy, and the classification results are shown in Table 3. Figure 14 is a histogram of the correctness of image recognition in the mining process of different algorithms when $R = 3$ and $n = 8$. Figure 15 is a histogram of the correctness of image recognition of mining processes with different algorithms when $R = 4$ and $n = 8$.

It can be seen from the classification results that the classification accuracy of the simulated annealing algorithm is up to 86.02%. This is because the characteristic information of the simulated annealing and the dispersion distribution information in the local dispersion mode are fused by the simulated annealing algorithm. Among other algorithms, the MS-PLPCM algorithm makes relatively full use of local information and pattern distribution information, and its classification accuracy is also high, but the MS-PLPCM algorithm also counts the features extracted by the pattern pair and approximates the distance to R. The classification accuracy of the U simulated annealing algorithm is lower than that of the RI simulated annealing algorithm. In addition, even in the nonuniform mode of the data set, it also indicates that the grouping contains information for classification. Because the simulated annealing V algorithm integrates the dispersion of local feature information into simulated annealing statistics, it has higher accuracy than previous algorithms. Disc simulated annealing algorithm integrates Fisher's discriminative idea, but the use of classification information is limited to the level of the number of local patterns, the use of class information is not ideal, and sometimes the key information is lost, so the classification accuracy is not higher compared with other algorithms.

4. Conclusion

In this paper, a mining engineering image feature extraction algorithm based on simulated annealing algorithm is proposed. The forward propagation and backward propagation algorithms are used to minimize the loss function, continuously update the bias and weight, repeatedly iterate training to obtain better parameters, and finally use the learned model for image recognition. Simulated annealing algorithm has the feature of automatic learning. Its advantage is to combine image feature extraction and classification, and exert its performance through mutual feedback adjustment, while the traditional methods are separated. Simulated annealing algorithm solves the bottleneck problems such as low recognition degree and long algorithm training time in traditional image recognition. It makes good use of the massive image data of the Internet, and the rapid development of computer hardware and software is enough to meet the complex calculation of the algorithm. This method can solve the inaccurate local binary recognition of the traditional simulated annealing algorithm and can strengthen the ability to explain the characteristics of mining engineering images. It not only improves the robustness of the algorithm, but also greatly improves the efficiency and real-time performance of the algorithm. Finally, the experimental results show that this algorithm can accurately extract the image features of mining engineering images and has better recognition rate and accuracy than other algorithms.

Data Availability

The data used to support the findings of this study are available from the corresponding author upon request.

Conflicts of Interest

The authors declare no conflicts of interest.

Acknowledgments

This research study is sponsored by the Natural Science Foundation of Heilongjiang Province. The project number is LH2020E110 2020-KYYWF-0523. Thank the project for supporting this article!

References

[1] Y. Zhao and Z. G. Zhang, "Mechanical response features and failure process of soft surrounding rock around deeply buried three-centered arch tunnel," *Journal of Central South University*, vol. 22, no. 10, pp. 4064–4073, 2015.

[2] W. Yu and K. Li, "Deformation mechanism and control technology of surrounding rock in the deep-buried large-span chamber," *Geofluids*, vol. 2020, 22 pages, 2020.

[3] C. Zhao, Y. Li, G. Liu, and X. Meng, "Mechanism analysis and control technology of surrounding rock failure in deep soft rock roadway," *Engineering Failure Analysis*, vol. 115, no. 2, p. 104611, 2020.

[4] W. Mu, L. Li, D. Chen, S. Wang, and F. Xiao, "Long-term deformation and control structure of rheological tunnels based on numerical simulation and on-site monitoring," *Engineering Failure Analysis*, vol. 118, no. 2, p. 104928, 2020.

[5] K. Janusz, T. Zvonko, and Z. Slobodan, "The soft rock socketed monopile with creep effects – a reliability approach based on wavelet neural networks," *Archives of Mining Sciences*, vol. 61, no. 3, pp. 571–585, 2016.

[6] N. S. Akbar and Z. H. Khan, "Rheological analysis of cnt suspended nanofluid with variable viscosity: numerical solution," *Communications in Theoretical Physics*, vol. 67, no. 6, pp. 681–687, 2017.

[7] X. Hu, Z. Zhou, H. Chen, and Y. Ren, "Seismic fragility analysis of tunnels with different buried depths in a soft soil," *Sustainability*, vol. 12, no. 3, pp. 892–1140, 2020.

[8] P. Shan and W. Sun, "Analysis of thermal effect around an underground storage cavern with a combined three-dimensional indirect boundary element method," *Engineering Analysis with Boundary Elements*, vol. 95, pp. 255–265, 2018.

[9] D. Sandanayake, E. Topal, and M. A. Asad, "A heuristic approach to optimal design of an underground mine stope layout," *Applied Soft Computing*, vol. 30, pp. 595–603, 2015.

[10] J. Menendez, J. Loredo, M. G. Vega, and J. Oro, "Energy storage in underground coal mines in nw Spain: assessment of an underground lower water reservoir and preliminary energy balance," *Renewable Energy*, vol. 134, pp. 1381–1391, 2019.

[11] W. Chen, J. Wang, and C. Wang, "Study of risk evaluation for complex projects under BIM and IPD collaborative pattern based on neighborhood rough sets," *Tehnicki Vjesnik-Technical Gazette*, vol. 27, no. 2, pp. 444–449, 2020.

[12] Y. A. Chirkunov and Y. L. Skolubovich, "Nonlinear three-dimensional diffusion models of porous medium in the presence of non-stationary source or absorption and some exact solutions," *International Journal of Non-linear Mechanics*, vol. 106, pp. 29–37, 2018.

[13] X. D. Song, H. Wu, F. Liu, J. Tian, and G. L. Zhang, "Three-dimensional mapping of organic carbon using piecewise depth functions in the red soil critical zone observatory," *Soil Science Society of America Journal*, vol. 83, no. 3, pp. 687–696, 2019.

[14] B. Rupnik, D. Kragelj, S. Šinko, and T. Kramberger, "Distributed energy resource operation analysis using discrete event-simulation," *Tehnicki vjesnik-Technical Gazette*, vol. 27, no. 3, pp. 860–867, 2020.

[15] A. Jahanbakhshzadeh, M. Aubertin, and L. Li, "Three-dimensional stress state in inclined backfilled stopes obtained from numerical simulations and new closed-form solution," *Canadian Geotechnical Journal*, vol. 55, no. 6, pp. 810–828, 2018.

[16] A. Kapahi and H. S. Udaykumar, "Three-dimensional simulations of dynamics of void collapse in energetic materials," *Shock Waves*, vol. 25, no. 2, pp. 177–187, 2015.

[17] G. Prerna and S. David, "Three-dimensional multicomponent vesicles: dynamics & influence of material properties," *Soft Matter*, vol. 14, no. 1, pp. 1–7, 2018.